Dual-Band Wearable Textile Antenna on an EBG Substrate

Shaozhen Zhu, *Student Member, IEEE*, and Richard Langley

***Abstract*—Performance of a dual-band coplanar patch antenna integrated with an electromagnetic band gap substrate is described. The antenna structure is made from common clothing fabrics and operates at the 2.45 and 5 GHz wireless bands. The design of the coplanar antenna, band gap substrate, and their integration is presented. The band gap array consists of just 3×3 elements but reduces radiation into the body by over 10 dB and improves the antenna gain by 3 dB. The performance of the antenna under bending conditions and when placed on the human body are presented.**

***Index Terms*—Body-worn antennas, dual-band antennas, electromagnetic band-gap (EBG) materials, printed antennas, textile antennas.**

I. Introduction

THERE is currently much interest in body-worn communication systems whether for on-body communication or communication off body to fixed and mobile networks. Such systems are of interest for detecting motion on the body during exercise, monitoring functions such as heart rate and blood pressure, use by the emergency services, and for general network connection. Consequently, antennas for applications such as airwave at 400 MHz, mobile telephones 800–2200 MHz and network communications at 2.45 GHz and 5–6 GHz are of interest. Body-worn antennas may be made from textiles [1]–[5] and attached on body or into clothing, or may be worn as a button antenna [6]. Authors have reported single frequency band wearable antennas [1]–[4] demonstrating acceptable performance at low cost. Later, dual frequency band designs have emerged allowing mobile network connection [6]–[8]. More recently an antenna incorporating a single-frequency electromagnetic band-gap material (EBGs) integrated into the design has been reported [9]. EBGs offer the potential advantage of reducing the backward radiation from the antenna and hence a reduction in the radiation absorbed by the body [10]. One study has reported on the electromagnetic properties of some textiles [11] and the effect of bending such antennas [12], an important problem for flexible body-worn antennas.

In this paper, we provide further results from a study of a dual-band textile antenna incorporating an EBG surface that was originally outlined in [13]. This antenna can be worn within clothing and covers the 2.45 GHz and the 5 GHz wireless networking bands. Construction of the antenna is based on a coplanar stripline feeding a coplanar patch antenna, giving a much wider operating bandwidth and more flexible band spacing than is possible from a dual-band microstrip patch antenna while maintaining the front to back ratio. These antennas are to be placed against the body and hence it is desirable to reduce the backward scattered radiation as much as possible. The antenna has been integrated with a dual-band EBG material to act as a high-impedance surface (HIS) to reduce back radiation and make the antenna tolerant to positioning on the body. The performance of the coplanar antenna and the dual-band EBG are presented and compared with a dual-band microstrip patch antenna. The antennas are conformal and manufactured from flexible materials that are readily hidden or sewn into items of clothing. The materials used are commonly found in clothing products and range from felts and cloths to leather fabrics. The electromagnetic properties of common textiles have been measured and are presented. The conducting components, coplanar feed line, patch antenna, and ground plane, are manufactured from a woven conducting fabric "Zelt." At this prototype stage, the antenna was constructed by hand cutting the conductive material accurately and attaching the components to a layer of thin felt material 1.1 mm thick with $\varepsilon_{\mathrm{r}} = 1.38$ and $\tan\delta = 0.02$ either by stitching them together or by using a very thin layer of adhesive. Later laser cut elements were used although no significant differences were noted in performance when compared to the hand cut prototypes. The antennas and band-gap high-impedance surfaces were designed and simulated using CST Microwave studio software and measurements were carried out to verify the results. Results are reported for the antenna bent around two formers in the E-plane and H-plane of the antenna and for the antennas placed on the human body. Specific absorption rate measurements and simulations were also carried out.

II. Fabric Characterization

In order to design textile-based antennas the electromagnetic properties of the materials must be known at the operational frequency bands. In this project, the dielectric properties of some common textile and leather materials were measured through a transmission/reflection waveguide method. The measurement setup was based on an HP 8720D network analyzer and a rectangular waveguide10 system (two identical waveguide cavities with transition parts, a shorting plate and a waveguide sample holder). The operating frequency range of the waveguide 10 system was 2.60–3.95 GHz. Six fabric samples and two reference solid samples (Perspex and PTFE) were measured. All the

Manuscript received December 18, 2007; revised October 28, 2008. Current version published April 08, 2009.

The authors are with the Department of Department of Electronic and Electrical Engineering, University of Sheffield, Sheffield S10 2TN, U.K. (e-mail: s.zhu@sheffield.ac.uk; r.j.langley@sheffield.ac.uk).

Color versions of one or more of the figures in this paper are available online at http://ieeexplore.ieee.org

Digital Object Identifier 10.1109/TAP.2009.2014527

TABLE I
AVERAGE RESULTS OF THE DIELECTRIC CONSTANT FOR EACH MATERIAL

Material	Silk	Tween	Panama	Moleskin	felt	fleece	PTFE	Perspex
Single layer thickness (mm)	0.58	0.685	0.347	1.17	1.1	2.55	11.66	11.67
Permittivity	1.75	1.69	2.12	1.45	1.38	1.17	2.05	2.57
Loss tangent	0.012	0.0084	0.018	0.05	0.023	0.0035	0.0017	0.008

fabrics were purchased from a department store and are very commonly used in clothing. The samples were cut to fit the waveguide aperture tested as single layers and in multiple layers.

Table I summarizes the bulk dielectric properties of the materials. The reference samples PTFE and Perspex give permittivity and loss tangent values that are within the expected ranges. The textiles have permittivities in the range 1.17 to 2.12 and acceptable loss tangents even in the worst case of moleskin at 0.05. The fabrics therefore present no major problems for antenna performance at these frequencies. In another study, leather materials were also characterized and the relative dielectric constants varied from 2.5 to 2.8 with loss tangents between 0.035 and 0.073. Several antennas have been tested on leather substrates with acceptable performance. Here, we concentrate on textiles rather than leather.

Having established that many textiles are suitable for use as antenna substrates an electrically conductive fabric for the ground plane as well as for the antenna patches was required. For the purposes of a textile antenna design, a conductive fabric needs to satisfy the following requirements:

- a low and stable electrical resistance ($\leq$1 ohm/square) is desired to minimize losses;
- the material must be homogeneous over the antenna area, and the variance of the resistance through the material should be small;
- the fabric should be flexible such that the antenna can be deformed when worn;
- the fabric should be inelastic, as the electrical property of elastic fabrics might change when stretching or bending.

The conducting material "Zelt"' has a high-quality nylon based substrate and is plated with copper and tin with a conductivity of 1 e + 006 S/m. Its thickness is 0.06 mm with a manufacturer's surface resistivity specification lower than 0.01 ohm/square, which is excellent for creating efficient antennas and RF circuits at wireless communication frequencies. Also Zelt fabric is durable, tear resistant, and is easy to form and handle. From a manufacturing point of view, it can be cut using laser ablation into a precise shape, also it can conform to any shape and be sewn like ordinary fabric to make highly effective clothing structures. Therefore, for all the antennas and structures used in this project, the woven conductive fabric, Zelt, was used. In this project most of the structures were hand cut and either sewn together or tacked to each other using a very thin spray adhesive. No losses were detected due to the adhesive layer.

III. DESIGN OF DUAL-BAND FABRIC ANTENNAS

The dual-band antenna required for this project needed to cover the frequency bands of 2.45 GHz band with a 2% bandwidth and the various wireless networking bands from 5.15–5.825 GHz. The bandwidth of the higher frequency at about 12% presents a significant challenge with a dual-band EBG. To achieve the bandwidth and keep the antenna as thin as possible a number of coplanar antennas were designed using CST software. Two such designs were briefly reported in [13] and [14]. One of these antennas is pictured in Fig. 1(a) where the antenna uses a felt substrate 1.1. mm thick and the complete geometry is shown in Fig. 2. The antenna is a coplanar design consisting of an inner patch surrounded by a parasitic rectangular ring element, surrounded by the normal ground of the coplanar feed line. The antenna measured 55 mm $\times$ 55 mm. A coplanar design was used as it has much wider bandwidth than a microstrip patch antenna. Simulations show the current excitation in Fig. 3 at two frequency bands of interest 2.45 and 5.8 GHz. The lower resonance at 2.45 GHz is largely due to the inner patch plus parasitic antenna ring around it resonating, while the inner patch fundamentally resonates at the upper frequency band.

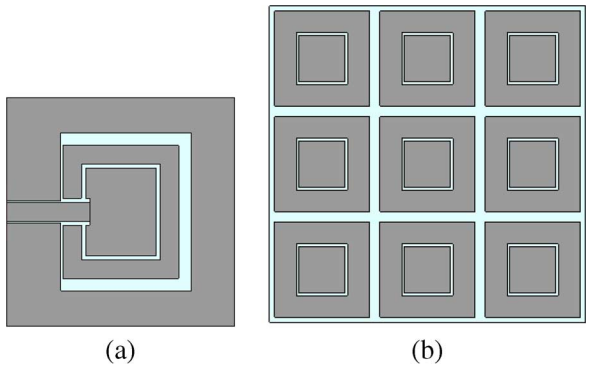

Fig. 1. Dual-band (a) coplanar antenna. (b) EBG substrate on felt material. (a) Antenna overall size 55 $\times$ 55 mm; inner patch 21 $\times$ 17 mm; inner gap 1 mm; inner square ring parasitic antenna 32 $\times$ 28 mm. Substrate thickness: 1.1 mm felt, permittivity $= 1.38$ Loss tangent $= 0.02$. (b) Fabric dual-band EBG structure (120 mm $\times$ 120 mm). Each cell: outer square 36 mm $\times$ 36 mm, inner square 17 mm $\times$ 17 mm. Substrate thickness over ground: 2.2 mm (felt as antenna).

The antenna impedance and radiation patterns were compared with similar coplanar antennas printed on FR4 substrate. Fig. 4 plots the simulated and measured reflection coefficient for the antennas on the felt and FR4 substrates. FR4 was chosen for comparison as it is a cheap and widely used substrate for commercial antennas. Simulation and measurement are in good agreement at the higher frequency band 5 GHz while at 2.45 GHz the measured bandwidths for a return loss of -10 dB at 19% are less than predicted at 28%. The radiation patterns of the antennas on the two substrates were very similar, but the gain of the felt-based antenna was 0.5 dB higher. Radiation

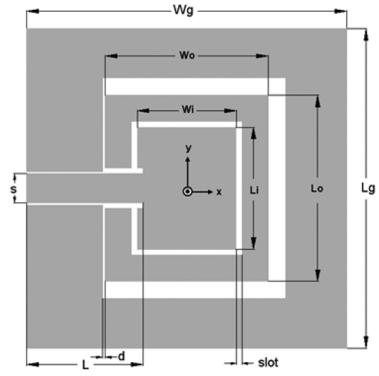

Parameters	Value (mm)
Lg, Wg	55
Lo	32
Wo	28
Li	21
Wi	17
s	5

Table 1. Antenna dimensions

Fig. 2. Dual-band CPW-fed fabric antenna geometry. (a) Top view. (b) Side view.

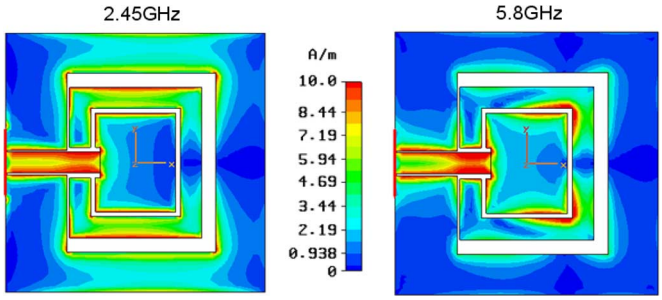

Fig. 3. Surface current distribution of the CPW antenna at 2.45 and 5.8 GHz.

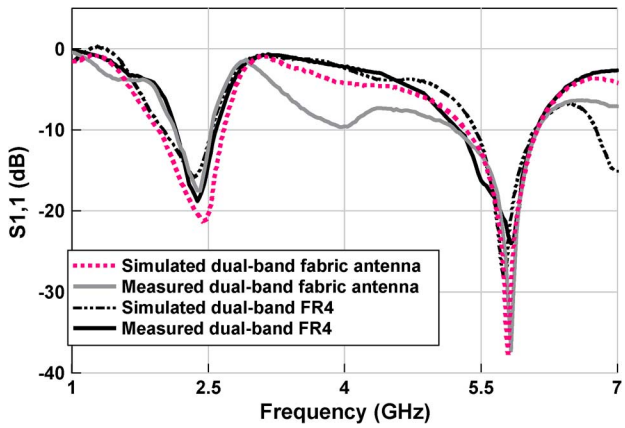

Fig. 4. Simulated and measured reflection coefficient comparison.

patterns in the E and H-planes are plotted in Fig. 5 at 2.45 GHz, 5.2 GHz, and 5.8 GHz together with those for the antenna with the EBG which are described later. The radiation patterns for the antenna alone at each frequency band are as expected from a coplanar patch antenna having radiation in both the forward and reverse directions.

IV. Design of Dual-Band High-Impedance Surface

There are many candidate geometries for the design of a dual frequency band HIS such as convoluted elements, pseudo-fractals, bow tie elements, etc. A double concentric square band gap design was investigated as this has been widely used in FSS designs [15] and was a relatively simple structure to fabricate as part of a textile antenna. No vias were used in the design as these are not needed for high-impedance surfaces and even without them a degree of surface wave suppression was obtained. The HIS was constructed on 2.2-mm-thick felt and the basic cell dimensions are shown in Fig. 6. The resonances of this dual-band EBG are determined by the geometry. The transmission response creates two 0° reflection phase points at the reflection band corresponding to the inner square patch and outer loop. The structure is designed so that the null points of the EBG reflection phase approximately coincides with 2.45 GHz and 5.5 GHz. This may require adjustment as when the HIS is integrated with the antenna these bands tend to shift slightly. The performance of the structure was computed using CST Microwave Studio, and the optimized dimensions for the concentric square EBG are depicted in Fig. 6. Simulation has shown that increasing the gap $\mathbf{g}$ between each element raises the resonance at each band while increasing the elements length $\mathbf{L_o}$, $\mathbf{L_i}$ lowers the resonant point at the corresponding band. The slot width s between the inner patch and the outer loop can be used to control the upper resonant band. The surface current flows at both frequencies are distributed in Fig. 7. It is clear that more currents are induced in the outer loop at 2.45 GHz and the currents are concentrated in the inner patch at 5.8 GHz.

To experimentally verify the surface wave transmission behaviour of the concentric square EBG, a 3×3 cell array was fabricated. The overall dual-band EBG structure measured 120×120 mm^2, consisting of just nine elements with each cell measuring 40×40 mm^2. A suspended strip line over the EBG ground plane was used to test the transmission response of the EM waves. The S_{21} was measured by connecting the strip line through the EBG array above the surface to the two coaxial ports: one as an exciting source and the other as a matched load. It is expected that for frequencies within the band gap of the structure, the EBG ground plane will stop the transmission of a wave along the stripline resulting in the reduction of S_{21} at a certain band of frequencies indicating the band gap position. Fig. 8. shows the measured S_{21} of the EBG surface. The simulated reflected phase response is also plotted for comparison. From the S_{21} plot the band gaps are centred at approximately 2.4 and 6.2 GHz. The in-phase reflection predicts the zero phase reflection at 2.45 and 5.7 GHz, respectively. The reflection phase band gap is slightly different with the EM wave suppression band gap for the designed EBG structure. This is because the suspended strip supports a quasi TEM mode with the dominant electric field component normal to the ground plane, while the normally incident plane wave is associated with the tangential component of the electric field.

V. Integration of Dual-Band Textile Antenna and HIS

The EBG array was designed to act as a high-impedance plane for the low profile antenna, to reduce the backward scattering wave towards the body and possibly minimize the cou-

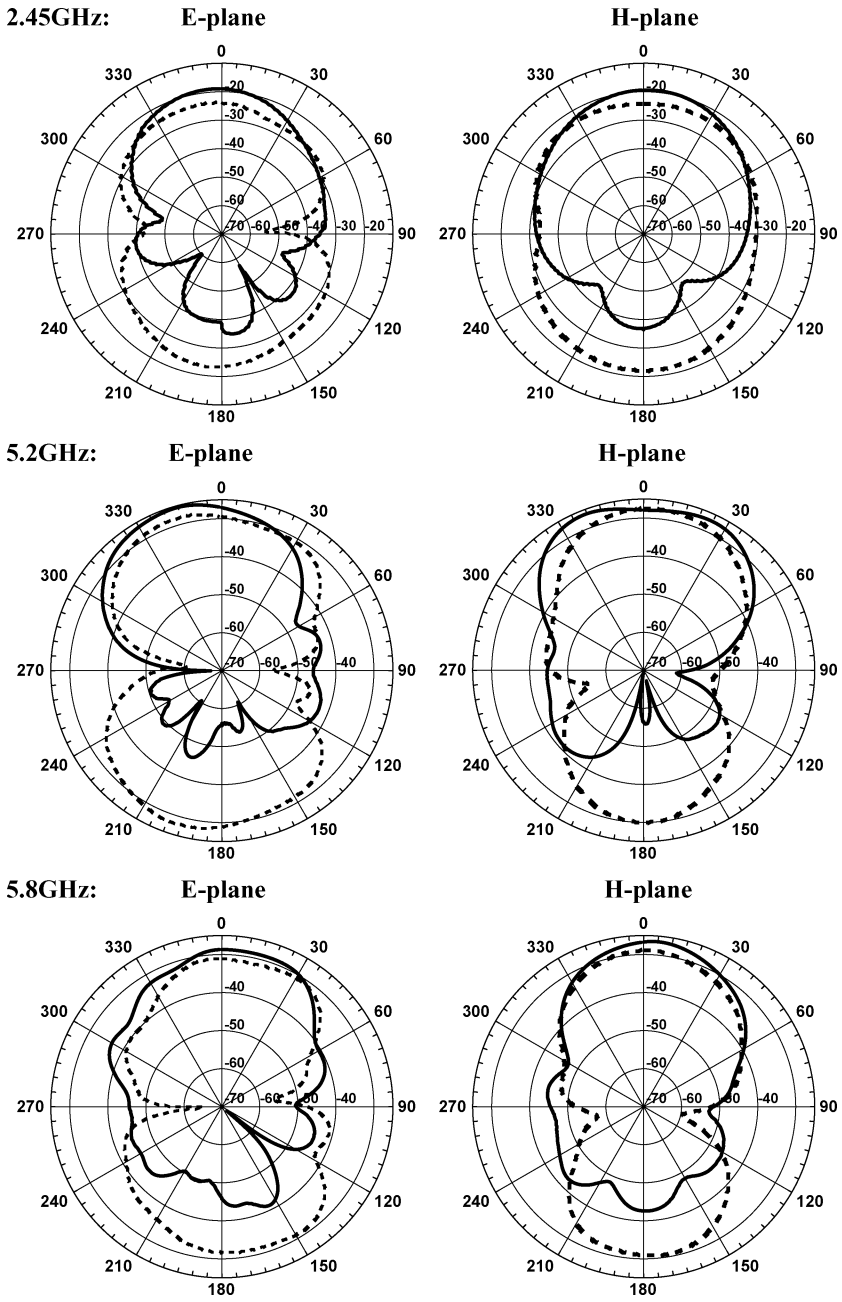

Fig. 5. Measured E- and H-plane radiation patterns at each frequency band.

pling between an antenna and other nearby antennas. In this section, the dual-band fabric CPW antenna and the 3×3 fabric EBG array are integrated. The complete integrated antenna is shown in Fig. 9. A thin 1-mm Rohacell ($\varepsilon_{\rm r} = 1.006$) layer is employed between the antenna and the EBG plane to prevent the antenna connector touching the elements. In practice the coplanar feed line would be extended across to the edge of the EBG. The overall thickness of the EBG antenna is 4.48 mm, which is about 0.036λ for the 2.45-GHz band. Two structures were tested, one used sellotape to keep the antenna on the EBG while in the other the antenna was sewn onto the EBG. Measurements were in good agreement and no significant differences in the performance were noticeable. The current distributions calculated for the antenna are plotted in Fig. 10 at 2.45 and 5.7 GHz. At the lower frequency band, the predominant current excitation is to be found on the antenna and less excitation than expected over the HIS. Interestingly even for this array of just 3×3 elements the current excitation over the HIS was about 8 dB down on the antenna peak excitation. At the high frequency band, the current excitation is largely confined to the antenna and the three HIS elements along the feed plane with very low excitation of the remaining elements.

The simulation and measurement results of the reflection coefficient for the complete antenna/EBG combination are plotted in Fig. 11 together with those for the coplanar antenna alone. The accuracy in the manufacture of the antenna reported here

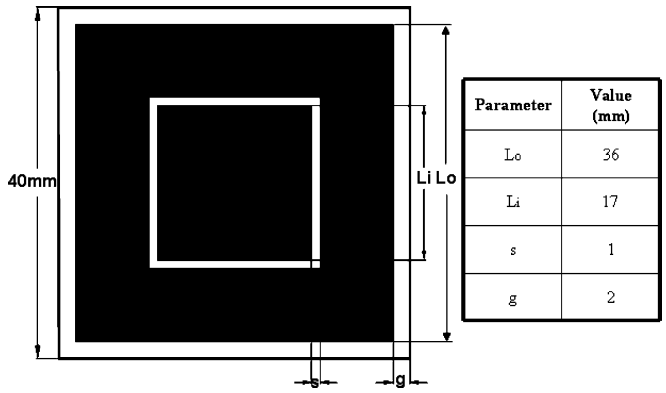

Parameter	Value (mm)
Lo	36
Li	17
s	1
g	2

Fig. 6. Schematic diagram of front view of concentric square EBG.

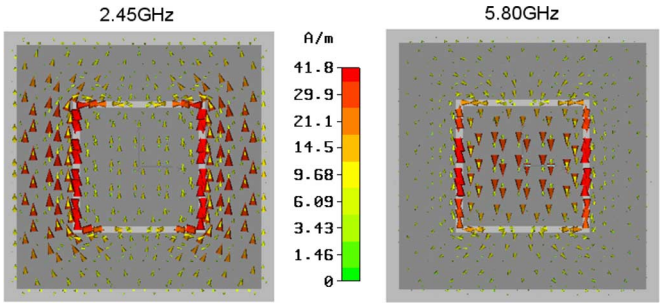

Fig. 7. Surface current flows for a single cell at 2.45 GHz and 5.8 GHz.

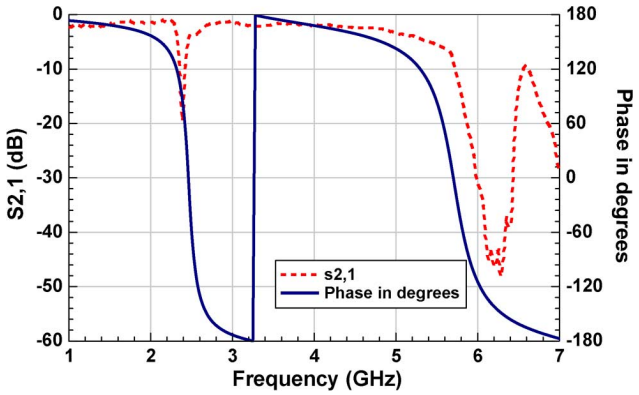

Fig. 8. Simulated and measured band gap response of double square HIS.

Calculated reflection phase

Measured S21 over surface

has been improved significantly compared to the original work in [13] and consequently the return loss at the upper frequency band near 5.7 GHz differs from that presented in [13]. Both the simulation and the measurements for the integrated structure show a bandwidth of 4% at the lower resonance band, this is reduced significantly when compared with the coplanar antenna which has a bandwidth of 17%. At the higher frequency band, the resonances are in broad agreement for simulation and the measurement, while the −10 dB bandwidth at 12% (5.4 to 6.15 GHz) for the measurement is much wider than that of the simulation at 8%. For the coplanar antenna the upper frequency bandwidth was 16%. The bandwidths for an equivalent microstrip antenna were 2.5% and 4.6% respectively at the two

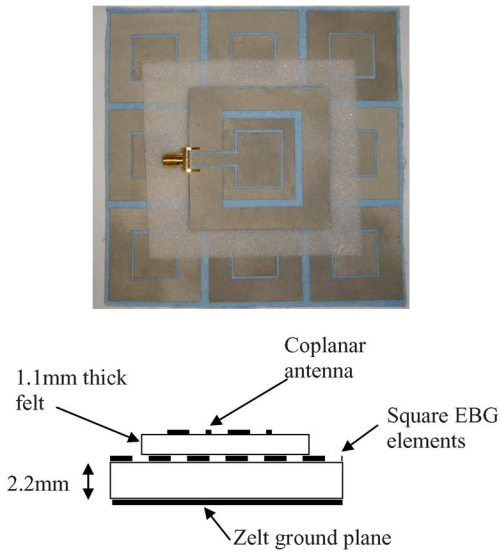

Fig. 9. Dual-band coplanar antenna on EBG plane.

frequency bands. Fig. 11 shows how important it is to design the antenna and band gap surface as a single integrated structure as the higher frequency band center has shifted upwards to 5.8 GHz. The integrated antenna was tested at 5.2 GHz even though the impedance match could be improved slightly by rectifying this.

Finally the radiation patterns measured at 2.45, 5.2, and 5.8 GHz are shown in Fig. 5 in the E- and H-planes for both the coplanar antenna alone and integrated with the HIS. The coplanar antenna without the EBG backing has a dipole like radiation pattern that is fairly omnidirectional and hence radiates into the body quite significantly. Placing the EBG behind the antenna considerably reduces the back radiation by at least 12 dB at the lower frequency band while improving the gain by up to 3 dB in a direction away from the body thus demonstrating the benefits of an EBG based antenna. The higher frequency radiation patterns showed the same general trend of improved gain and less back radiation even for this small array of just nine elements. Examining the surface current distributions in Fig. 10 it is surprising that the front to back radiation was not improved even further as generally the current is low on the EBG. However in the feed plane it was still significant and in addition the fabrication accuracy of the textile antenna was far from perfect and this may also account for a reduced performance. The gain for the integrated antenna was measured at 6.4 dBi at 2.45 GHz and 7.6 dBi at 5.8 GHz compared with 3.9 dBi and 5.2 dBi for the coplanar antenna, respectively. The gain of the equivalent microstrip patch antenna was 5.2 dBi at 2.45 GHz and −0.3 dBi at 5.8 GHz. The same integrated antennas were fabricated on FR4 material for comparison with the fabric based ones. In this case there was no significant measured difference in the gains of either antenna regardless of material.

VI. Antenna on Human Body

Installing the integrated antenna onto the human body as a body-worn system will give rise to a number of potential

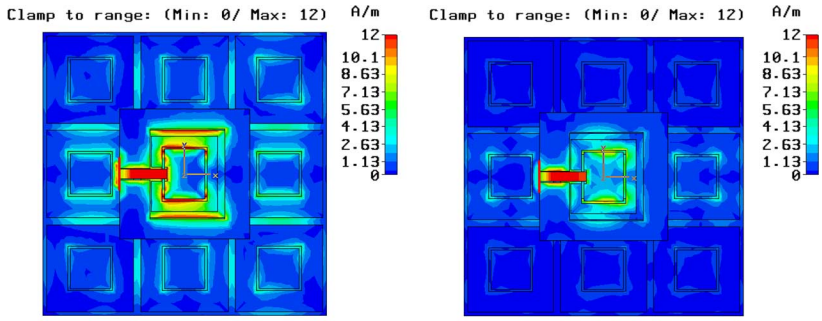

Fig. 10. Simulated current distributions over the combined antenna at two frequencies.(a) 2.45 GHz. (b) 5.7 GHz.

TABLE II
SIMULATED AND MEASURED SAR COMPARISON

Peak SAR values W/Kg: a comparison between simulation and measurement				
1800MHz	**1 gram tissue**		**10 gram tissue**	
	Simulation	**Measurement**	**Simulation**	**Measurement**
CPW antenna	**11.47**	**12.87**	**7.18**	**7.96**
EBG antenna	**0.48**	**0.90**	**0.31**	**0.42**

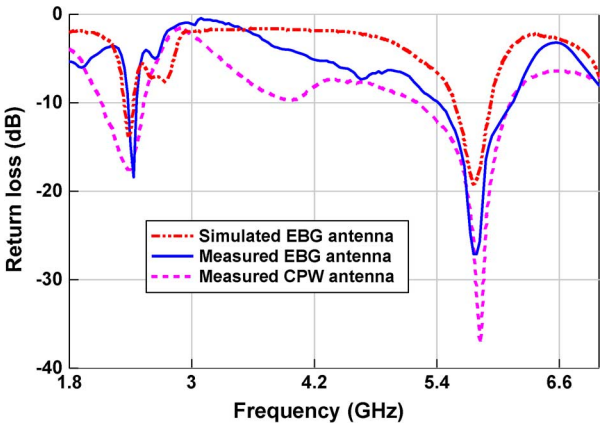

Fig. 11. Measured and simulated reflection coefficient for integrated antenna/ EBG.

problems. The antenna will be bent around the body, potentially crumpled, interact with the body and washed unless waterproofed in some manner. Of interest is also the specific absorption rate (SAR) performance into the body. These factors are considered in this section.

A. *Specific Absorption Rate*

Wearable fabric antennas are designed for on-body communications, which means that the antenna needs to be operating in the vicinity of the human body. Therefore, the SAR is an essential factor to evaluate when the antenna is excited on the body. The SAR was measured at the University of Loughborough using their DASY4 system [16]. This system was only calibrated for 1800 MHz rather than 2.45 and 5.5 GHz. To overcome the calibration problem an identical single band coplanar fed fabric antenna was designed over a 3 $\times$ 3 cells EBG array for 1800-MHz operation. The integrated antenna was then built and the SAR measured on the DASY4 system. Simulations using CST were performed and compared with measurements in Table II. The simulation model was a two layer liquid as per the DASY4 phantom.

The EBG antenna has reduced SAR by 96.5% for 1 gram (U.S. standard) and 97.3% for 10 g tissues (EU standard) in simulation. This was in good agreement with the measurements. The overall SAR values are slightly lower from simulation than those of the measurement. This could be due to the approximate phantom size modeled in the simulation and that, unlike the ideal environment in software, the conditions under measurement are more complicated. Effects of the connectors, cables, surrounding devices and temperature also need to be taken into account.

Based on the results at 1800 MHz and the acceptable agreement between simulation and measurement, the model was used to calculate the SAR values for the dual-band WLAN antenna and EBG integrated antenna using CST software. In addition the results are compared with those for a dual-band microstrip patch antenna, using a felt substrate 1.1 mm thick, operating at the same frequencies on a ground plane the same size as the EBG used with the coplanar antenna. It was not possible to design a dual-band microstrip antenna operating at the same frequencies on a felt substrate 3.3 mm thick. The distance between the human phantom and the antenna top surface was 5.3 mm in all cases. This gives a direct comparison of the performance of the EBG antenna with that of a ground plane based antenna

TABLE III
TISSUE PARAMETERS SET UP IN THE SIMULATION

	shell			liquid		
	ε_r	Loss tangent	Densityρ [kg/m3]	ε_r	conductivity σ [S/m]	Densityρ [kg/m3]
2.45GHz	3.3	0.03	1000	39.2	1.8	1000
5.8GHz	3	0.035	1000	35.114	3.717	1000

TABLE IV
SIMULATED SAR OF WLAN ANTENNAS ON THE RECTANGULAR LIQUID BODY

Peak SAR values W/Kg-dual band WLAN antennas						
	Size (mm^2)	Distance from patch antenna to body	2.45GHz		5.8GHz	
			1g tissue	10g tissue	1g tissue	10g tissue
CPW antenna	55×55	5.3mm	13.85	7.819	20.29	6.808
CPW antenna on EBG	120×120	5.3mm	0.079	0.043	0.127	0.090
Microstrip antenna	120×120	5.3mm	0.10	0.043	0.143	0.097

of the same dimensions. An alternative comparison would be to remove the EBG patches from the integrated coplanar antenna while keeping the antenna over the ground plane. However, the ground plane under the coplanar antenna (3.3 mm away) effectively shorts it out at both frequencies although there was a resonance at 6.2 GHz which is discussed later. The values for the liquid and the shell for each frequency are listed in Table III, and the computed peak SAR results are summarized in Table IV.

The results clearly demonstrate that the EBG has brought the power absorption down significantly compared with the CPW antenna alone and this is to be expected as the EBG antenna is directional. It is interesting to note that the SAR values for the microstrip antenna are similar to those for the EBG antenna at both frequency bands showing that the EBG is suppressing surface waves across the substrate that would otherwise radiate backwards into the body. Although the real measurement can not be carried out, the simulation gives a reliable indication of the benefits of the EBG. SAR values for the coplanar antenna over the ground plane with the EBG patches removed were computed at 6.2 GHz where the structure now resonated. There was no resonance at 2.45 GHz. The 10-g value was 0.020 W/kg compared with 0.090 W/kg with the EBG inserted. However, the antenna was no longer practical operating over a single band at a higher frequency.

Further simulations have been carried out using a multilayer model where the torso consists of four main layers of body tissues: bone, fluid, muscle, and skin. These support the conclusions obtained for the two-layer model.

B. Bending the Antenna

An antenna's performance under bending conditions is one of the important factors for wearable applications. Under an on-body environment it is difficult to keep the antenna in a flat condition especially for elements made of textile materials. In order to evaluate the antenna and EBG when placed in an on-body environment the antennas were tested in two ways, first on polystyrene formers and secondly on a human body. Polystyrene formers of two different diameters of 80 and 140 mm, respectively, were chosen, corresponding approximately to the typical size of a human arm and leg; see Fig. 12. These diameters are to some extent arbitrary but the 80-mm-diameter bend is a reasonably severe test. The return loss and radiation patterns were measured to evaluate the performance for both E-plane and H-plane bending. Initially, the performance of the dual-band antenna alone was evaluated but no significant changes were noted in either the return loss or radiation patterns as this is a relatively small object just 55 mm across. Fig. 12 shows the reflection coefficient for the integrated EBG antenna as a planar antenna and

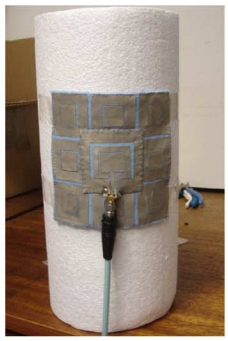

(a)

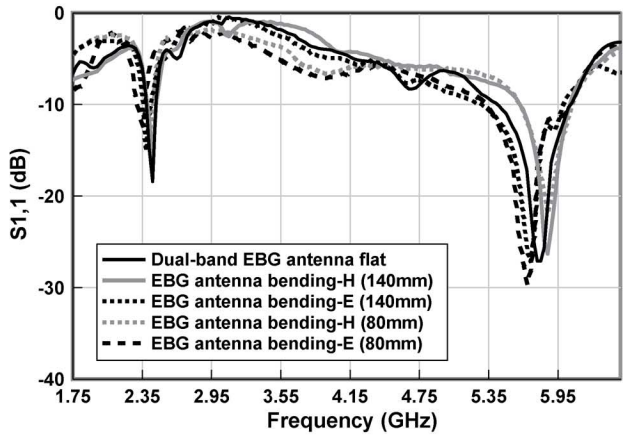

(b)

Fig. 12. Bending integrated antenna in the E-plane and H-plane—reflection coeficient. (a) Antenna mounted on polystyrene former. (b) Measured reflection coefficient for antenna on former.

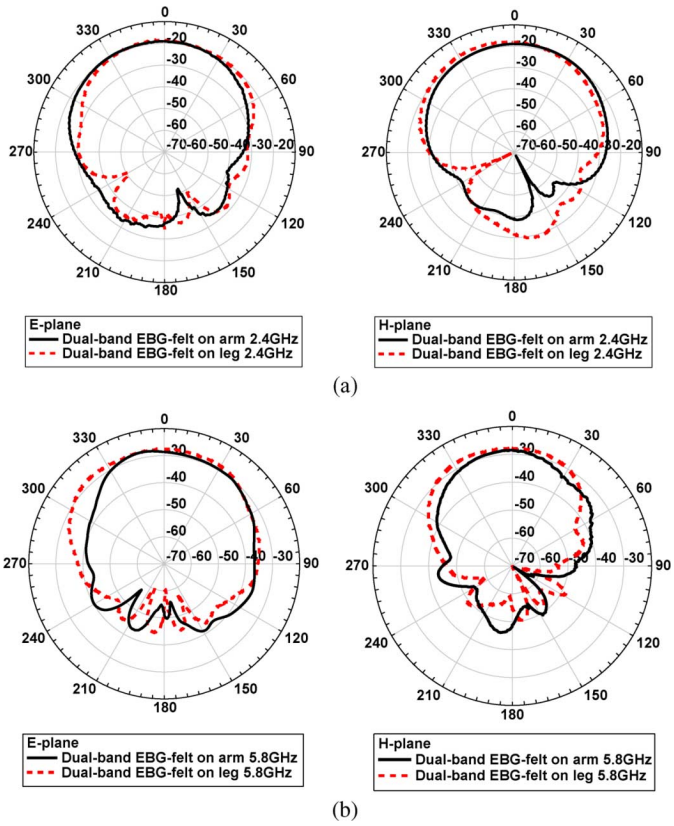

Fig. 13. Radiation patterns measured for antenna on 140 and 80 mm formers in the E-plane and H-plane. (a) 2.45 GHz. (b) 5.8 GHz.

on the two formers in the two planes. At 2.45 GHz, there was a downward shift in the center resonant frequency of 50 MHz on the 80-mm smaller diameter former for the E-plane bend while for the H-plane bend this was just 20 MHz. Changes for the 140 mm former were very small, 10 MHz or less. The bandwidth remained the same in all cases. At the higher frequency band there was more shift in the resonant frequency but again no change in bandwidth. At the 5.8-GHz band Fig. 12 shows that the H-plane bend causes the resonance to move up in frequency by 75 MHz for the 80 mm former, and slightly less for the larger 140 mm former of about 65 MHz. For an E-plane bend, the resonance moves downward by 75 MHz for the 140 mm former and 120 MHz for the 80 mm former.

The radiation pattern plots in Fig. 13 show little variation over the planar antenna at 2.45 GHz in either plane except that there is more back radiation from the 140-mm-diameter H-plane measurement of about 6 dB when compared to the planar or 80 mm bending. This may be due to experimental error as there was no change in the backward radiation measured at the higher frequency of 5.8 GHz in either plane as seen in Figs. 13(c) and (d). However some differences in the radiation patterns are noticeable at 5.8 GHz at different angles but overall there is no significant change in the beamwidth or gain between the bent and planar antennas, this is true at both frequency bands. These differences may be due to the difficulty of mounting and aligning what are prototype antennas that are very flexible.

C. On-Body Measurements

The band gap structure provides reduced backwards radiation from the antenna, a lower SAR and hence the antenna should be tolerant to being placed on the body. In a series of experiments the antenna was placed on a human arm and thigh and measurements on the return loss and radiation patterns (at the lower frequency only) were carried out. In Fig. 14, the reflection coefficient is plotted for the EBG antenna in free space and when placed on three different parts of the body—the arm, thigh, and back. The antenna was placed directly onto the skin of the arm, onto a thin tight T shirt on the back and onto denim jeans on the thigh such that the bend was in the H-plane. When compared to the antenna alone the return loss remains the same for the antenna placed on the back at either frequency band. When placed on the thigh and arm there was a small shift upward in the resonant frequency of about 50 MHz, in agreement with the measurements on the polystyrene former. At the higher frequency band, there was an upward shift in the resonant frequency of 80 MHz on the thigh and about 120 MHz on the arm, again in agreement with the measurements on the former. In all cases the bandwidth was unchanged. In addition, radiation patterns have been measured at 2.45 GHz in an anechoic chamber with the antenna worn on a human body on the thigh in this case; see Fig. 15. These measurements were demanding to conduct as the first author had to stand on a large turntable during several measurements that took many minutes each, and where precise positioning and steadiness were difficult to achieve. However, the measurements give an indication of the performance of the

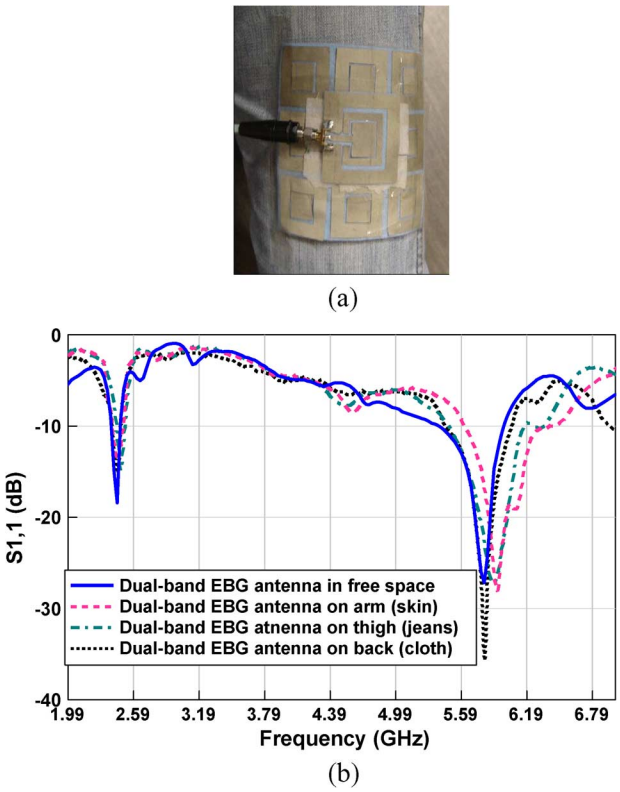

Fig. 14. Reflection coefficient of integrated antenna on a human body. (a) Antenna on thigh. (b) Reflection coefficient measured for different body locations.

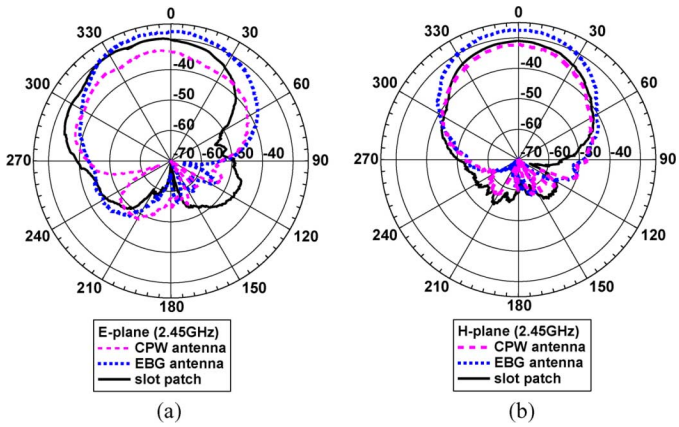

Fig. 15. Measured radiation patterns for three on-body antennas. (a) E-plane. (b) H-plane.

Coplanar waveguide antenna
Integrated CPW/EBG antenna
Patch antenna (reference)

antenna. The patterns are compared in Fig. 15 with those for the coplanar patch antenna alone, the integrated EBG antenna and a microstrip patch antenna with a ground plane the same size as the EBG antenna and used as a reference; see Table IV. It is noted that the integrated EBG antenna has the highest gain, about 3 dB more than the reference patch. The coplanar antenna without the EBG backing is loaded by the body materials and has a much reduced gain, about 6 dB lower than the integrated EBG antenna. The reference microstrip patch has a gain about 3 dB lower than the EBG antenna. The overall radiation patterns are similar if angular differences that probably relate to the difficult measurement conditions are ignored.

D. Washing Textile Antennas

Finally the performance of the integrated antenna was tested after and during a number of hand washing cycles to determine whether textile antennas could stand such basic rigors. The fabric used here was felt which potentially shrinks by about 3% after several washes. It is not known how the Zelt conductor fares but as a nylon based product it is unlikely to shrink. The antenna was washed and measured when in states of extreme wetness and dampness and finally when fully dried again. It can be reported that the performance before and after washing when fully dried remained unchanged. Dampness (about 5% water content by weight) caused a shift in the resonant frequency downwards by about 5% while the radiation patterns were unaltered but the gain reduced by 2 dB at the lower band and 3 dB at 5.8 GHz. Clearly other textile materials will have different washing properties and the best solution would be to waterproof the whole antenna to protect it.

VII. Conclusion

The paper has demonstrated a wearable coplanar antenna integrated with an EBG surface that operates at two frequency bands of interest for wireless network communications. The integrated antenna has operating bandwidths of 4% at 2.45 GHz and 16% at 5.5 GHz while an equivalent microstrip patch antenna has respective bandwidths of 2.5% and 4.6%. The electromagnetic properties of common textiles have been measured and shown to be acceptable for antenna manufacture. The EBG is used as a high impedance surface and consists of just 3 $\times$ 3 elements. Despite the small EBG structure the integrated EBG antenna has relatively low back radiation and reduces SAR values by a factor of up to 20 while having higher gain in directions away from the torso to improve communication performance. The SAR values calculated for the EBG based antenna were similar to those computed for a microstrip antenna at the same distance above the body with the same ground plane dimension indicating effective suppression of the surface waves. The gains of the body-worn antennas at both frequency bands are comparable with antennas printed on commercial FR4 substrates. Simulations are generally in good agreement with measurements. Measurements show that the antenna is tolerant to bending in either plane when shaped around both polystyrene formers and human arms and legs. Bending in the E-plane affects performance more than the H-plane, the most noticeable effect being a reduction in the resonant frequency of 2% in the worst case of the arm (diameter 80 mm), although the bandwidths are unchanged. Radiation patterns remained good and the antenna gain unchanged. The antenna was tolerant to being placed on a human body and the on-body measurements retained good return loss and radiation pattern performance.

Although not shown here the EBG also provides further isolation between adjacent antennas of up to 15 dB despite the fact

that the EBG elements have no vias, hence a planar periodic structure can still reduce surface wave coupling.

Overall, this paper has demonstrated that it is possible to manufacture dual frequency band textile antennas integrated with band gap surfaces that are tolerant to being placed on the body and that give a performance that is as good as conventionally manufactured antennas. The performance of the integrated antenna is superior to that of an equivalent microstrip patch antenna in terms of bandwidth and gain while having a similar front to back ratio.

ACKNOWLEDGMENT

We thank Dr Lee Ford for his assistance with the material parameter measurements and Dr Rob Edwards of Loughborough University for use of the DASY4 system for measuring the SAR parameters.

REFERENCES

[1] P. J. Massey, "Mobile phone antennas integrated within clothing," in *Proc. IEE 11th Int. Conf. Antennas Propag. (ICAP'01)*, Manchester, U.K., 2001, vol. 1, pp. 344–347.

[2] P. Salonen, M. Keskialammi, and L. Sydanheimo, "A low cost 2.45 GHz photonic band gap patch antenna for wearable systems," in *IEE 11th Int. Conf. Antennas Propag. (ICAP'01)*, Manchester, U.K., 2001, vol. 2, pp. 719–723.

[3] A. Tronquo, H. Rogier, C. Hertleer, and L. Van Langenhove, "Robust planar textile antenna for wireless body LANs operating in 2.45 GHz ISM band," *Electron. Lett.*, vol. 42, no. 3, pp. 142–143, 2006.

[4] M. Klemm and G. Troester, "Textile UWB antennas for wireless body area networks," *IEEE Trans. Antennas Propag.*, vol. 54, no. 11, pp. 3192–3197, Nov. 2006.

[5] , P. S. Hall and Y. Hao, Eds., *Antennas and Propagation for Body Centric Communications Systems*. Norwood, MA: Artech House, 2006.

[6] B. Sanz-Izquierdo, F. Huang, and J. C. Batchelor, "Convert dual band wearable button antenna," *IET Electron. Lett.*, vol. 42, no. 12, pp. 668–670, Jun. 2006.

[7] P. O. Salonen, Y. Rahmat-Samii, H. Hurme, and M. Kivikoski, "Dual-band wearable textile antenna," in *Proc. IEEE Antennas Propag. Int. Symp.*, 2004, vol. 1, pp. 463–467.

[8] E. C. Kohls *et al.*, "A multi-band body-worn antenna vest," in *Proc. IEEE Antennas Propag. Int. Symp.*, 2004, vol. 1, pp. 447–450.

[9] P. O. Salonen, F. Yang, Y. UCLA Rahmat-Samii, and M. Kivikoski, "WEBGA—Wearable electromagnetic band-gap antenna," in *Proc. IEEE Antennas Propagat. Int. Symp.*, 2004, vol. 1, pp. 455–459.

[10] D. F. Sievenpiper *et al.*, "High-impedance electromagnetic surfaces with a forbidden frequency band," *IEEE Trans. Microwave Theory and Techniques*, vol. 47, no. 11, pp. 2059–2074, Nov. 1999.

[11] P. Salonen, Y. Rahmat-Samii, M. Schaffrath, and M. Kivikoski, "Effect of textile materials on wearable antenna performance: A case study of GPS antennas," in *Proc. IEEE Antennas Propag. Soc. Int. Symp.*, 2004, vol. 1, pp. 459–462.

[12] P. O. Salonen and Y. Rahmat-Samii, "Textile antennas: Effect of antenna bending on input matching and impedance bandwidth," in *Proc. Eur. Conf. Antennas Propag., EuCap06*, France, Nov. 2006.

[13] S. Zhu and R. J. Langley, "Dual band wearable antennas over EBG substrate," *IET Electron. Lett.*, vol. 43, no. 3, pp. 141–143, Feb. 2007.

[14] L. Liu, S. Zhu, and R. J. Langley, "Dual band triangular patch antenna with modified ground plane," *IET Electron. Lett.*, vol. 43, pp. 140–141, Feb. 2007.

[15] R. J. Langley and E. A. Parker, "Double square frequency selective surfaces and their equivalent circuit," *Electron. Lett.*, vol. 19, pp. 675–677, 1983.

[16] *"DASY4 System Handbook,"* Schmid & Partner Engineering AG, DASY4 Manual V4.5, Mar. 2005.

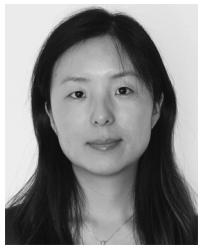

Shaozhen Zhu (S'06) received the M.S. degree in electronics engineering from University of Kent, Canterbury, U.K., in 2004 and the Ph.D. degree from the University of Sheffield, Sheffield, U.K., in 2008.

She is currently a Postdoctoral Researcher at the Department of Electronic and Electrical Engineering, University of Sheffield. Her research interests include miniaturized antenna and electromagnetic bandgap structures, metamaterial applications, flexible antenna for wearable applications, and medical implanted wireless communications.

Richard Langley received the B.Sc. and Ph.D. degrees from the University of Kent, Canterbury, U.K., 1971 and 1979, respectively.

He was a Professor of Antenna Systems at the University of Kent from 1994 to 2005 before moving to the University of Sheffield to become Head of the Communications Group. For many years, his main research was in the field of frequency selective surfaces applying them in the satellite and defence fields. This led to his interest in the development of novel electromagnetic band-gap surfaces applying them to compact antenna systems. Current research interests are hidden automotive antennas, multiband antennas for handsets and networks, miniature antennas, and components and reconfigurable systems. In 1997, he founded the European Technology Center for Harada Industries Japan, where he was Director of the Center until 2003 when he returned to academic life. His involvement with Harada Industries of Japan in developing new automotive antenna technologies has resulted in many patents.

Prof. Langley was Honorary Editor of IEE Proceedings Microwaves, Antennas, and Propagation from 1995 to 2004.